frontiers in Materials

ORIGINAL RESEARCH
published: 26 February 2021
doi: 10.3389/fmats.2020.629284

Flame Retarded Rigid Polyurethane Foams Composites Modified by Aluminum Diethylphosphinate and Expanded Graphite

Yuxiang Hu[1], Zijian Zhou[2], Shuisheng Li[1], Dong Yang[1], Shui Zhang[1] and Yakang Hou[1]*

[1]China Construction Fifth Engineering Division Co., Ltd., Changsha, China, [2]School of Architecture and Civil Engineering, Anhui University of Technology, Ma'anshan, China

Rigid polyurethane foam (RPUF) was an organic porous material, which was applied in many fields for excellent thermal insulation and mechanical properties, especially in building insulation. However, the poor fire performance significantly suppresses its further application. In this work, aluminum diethylphosphinate (ADP) combined with expanded graphite (EG) to form a synergistic flame retarded system, which was introduced to fabricate flame retarded rigid polyurethane foam composites (FR-RPUF) by one-step water-blown method. Furthermore, thermal insulation, thermal stability, fire performance, and decomposition products of RPUF and FR-RPUF composites were systematically investigated. It was found that FR-RPUF composites possessed LOI of 25.9 vol% with V-1 rating in UL-94 test when 10 php of ADP and 20 php of EG were added, which were better than RPUF composites with ADP or EG added alone. MCC test showed that RPUF/ADP24/EG6 had the lowest PHRR value of 159.85 W/g, which was 52.01 W/g lower than that of pure RPUF. Gas phase products investigation implied that the combination of ADP and EG could decrease toxic and combustible gases intensities, thus significantly enhancing fire safety of FR-RPUF composites. SEM test indicated that ADP and EG promoted the formation of dense and continuous char residue, which significantly inhibited heat and substance transfer in combustion, thus significantly enhancing fire performance of FR-RPUF composites.

Keywords: flame retarded, rigid polyurethane foams, aluminum diethylphosphinate, expanded graphite, thermal stability

OPEN ACCESS

Edited by:
Yongqian Shi,
Fuzhou University, China

Reviewed by:
Bihe Yuan,
Wuhan University of Technology, China
Gang Tang,
Anhui University of Technology, China
Weizhao Hu,
University of Science and Technology of China, China
Yuezhan Feng,
Zhengzhou University, China

****Correspondence:***
Dong Yang
ydcscec@hotmail.com

Specialty section:
This article was submitted to Polymeric and Composite Materials, a section of the journal Frontiers in Materials

Received: *14 November 2020*
Accepted: *16 December 2020*
Published: *26 February 2021*

Citation:
Hu Y, Zhou Z, Li S, Yang D, Zhang S and Hou Y (2021) Flame Retarded Rigid Polyurethane Foams Composites Modified by Aluminum Diethylphosphinate and Expanded Graphite. Front. Mater. 7:629284. doi: 10.3389/fmats.2020.629284

INTRODUCTION

Rigid polyurethane foams (RPUF), as a novel organic porous material, are widely applied in building, pipeline engineering, refrigerator, and other fields for its excellent thermal insulation performance and mechanical properties (Hejna et al., 2018; Wang et al., 2018; Li et al., 2020; Wang et al., 2020). However, RPUF is easily to be ignited and released kinds of toxic and combustible gases, which would result in heavy casualties in the fire (Barkoula et al., 2008; Liu and Wang, 2018). This shortcoming significantly restricts the further application of RPUF and RPUF composites in many fields, especially in building constructions. Thus, many researchers try to enhance flame retardancy of RPUF (Wang et al., 2018; Bhoyate et al., 2019). Usually, additive and reactive strategies are the common ways to enhance fire performance of RPUF and its composites. Reactive flame retarded

RPUF is fabricated by involving phosphorus-containing diols and polyols. This strategy is often limited for high cost and poor storage stability of phosphorus-containing diols and polyols. The most used way in engineering for fire retardancy of RPUF is additive strategy, which only simply incorporates flame retardant particles in the formation process of RPUF. Some typical flame retardants, such as expandable graphite (EG), ammonium polyphosphate (APP), aluminum hypophosphite (AHP), melamine polyphosphate (MPP), and steel slags (SS), are introduced to fabricate flame retarded RPUF composites. Chen et al. prepare RPUF/EG composites and systematically research structure and flame retardancy of the composites. It is found that 15 phr EG loading endowed LOI of 22.2 vol% for the composites with significantly decreased PHRR and THR value (Chen et al., 2019). Cheng et al. prepare polyurea microencapsulated ammonium polyphosphate (POAPP), which is further applied into RPUF/POAPP composites. It is observed that RPUF/POAPP20 with 20 wt% POAPP loading possessed LOI of 24.8 vol% with 33.9% decrease of PHRR value compared with virgin RPUF (Cheng et al., 2020). Tang et al. combine melamine polyphosphate with steel slag; 2.5 wt% of steel slag and 7.5 wt% of MPP made RPUF composites reach LOI of 24.0 vol% (Tang et al., 2020).

Metal hypophosphate, as a novel flame retardant, is widely used in enhancing fire performance of polymers, including polylactides, thermoplastic polyurethane, and polyamide (Tang et al., 2012; Zhou et al., 2019; Pan et al., 2020). Tang et al. report flame retarded polyurethane foam composites based on aluminum diethylphosphinate (ADP), in which 30 php ADP loading makes RPUF composites possess LOI of 23.0 vol% (Tang et al., 2020). However, because of porous structure, it is very hard to enhance fire performance of RPUF composites, and high loading of flame retardant will inhibit foam formation and be harmful to thermal insulation of the composites. Thus, it is meaningful to fabricate flame retardant RPUF composites with lower flame retardant loading. Synergism strategy can be a good way for solving this problem and many researches about synergistic effect in RPUF system are reported. Chen et al. systematically investigate synergistic effect of ionic liquid modified expandable graphite/3-(N-diphenyl phosphorous) amino-propyl triethoxysilane (IL-EG/DPES) in RPUF composites. It is reported that RPUF composites with 10 phpp IL-EG and10 phpp DPES presented best compressive strength and flame retardancy compared with RPUF with only DPES or IL-EG added (Chen et al., 2020). Han et al. (2020) fabricate flame retardant RPUF composites based on diethyl bis(2-hydroxyethyl) aminomethylphosphonate (DBHP) and organoclay (OMMT). It is found that the RPUF composites with OMMT and DBHP loading possessed significantly raised LOI value and UL94 rating, reduced heat release rate and total heat release, and increased char yields (Han et al., 2020). Akdogan et al. report the synergistic effect of expandable graphite (EG) and ammonium pentaborate octahydrate (APB) in RPUF composites. The flame retarded RPUF composite with 15 wt EG and 5 wt% APB loading possesses PHRR reduction of 57.5% and THR reduction of 42.8% compared with those of virgin RPUF (Akdogan et al., 2020).

Expandable graphite (EG) often plays its flame retardant role by generating worm-like structure, which could suppress mass and substance transfer in condensed phase. Metal hypophosphate salts (MHP) exhibit flame retardancy for generating lots of PO· radicals, which could quench H· and HO in gas phase. The combination of flame retardant effect in condensed phase and gas phase often results in excellent fire retardancy. However, there are a few reports about EG/MHP system applied in RPUF composites. In this work, expandable graphite (EG) is combined with aluminum diethylphosphinate (ADP) to form a novel synergistically flame retarded system, which is further introduced in RPUF. A series of RPUF/ADP/EG composites are fabricated by one-step water-blown method. Thermal stability, thermal insulation property, fire retardancy, and combustion properties of RPUF/ADP/EG composites are characterized by thermogravimetric analysis (TG), thermal conductivity meter, limiting oxygen index (LOI), and UL-94 vertical burning test, microscale combustion calorimetry (MCC), and cone calorimetry (CONE). The gaseous products of the composites are investigated by TG-FTIR. And also, the char residues of composites are researched by X-ray photoelectron spectroscopy (XPS) and scanning electron microscope (SEM).

EXPERIMENTAL SECTION

Materials

LY-4110 (viscosity: 2,500 mPa·s, hydroxyl number: 430 mg KOH/g, purity ≥99 wt%), triethylenediamine (A33, Purity 33 wt%), and silicone surfactant (AK880599, purity ≥99 wt %) were provided by Jiangsu Luyuan New Materials Co., Ltd, China. Polyaryl polymethylene isocyanate (PAPI, purity ≥99.9 wt%) was provided by Wanhua Chemical Group Co., Ltd, China. Dibutyltin dilaurate (LC, purity ≥99 wt%) was obtained from Air Products and Chemicals, Inc. Triethanolamine (TEOA, 99.9 wt%) was purchased from Sinopharm Chemical Reagent Co., Ltd, China. Distilled water used as a chemical blowing agent was made in our laboratory. Aluminum diethylphosphinate (ADP, purity ≥99 wt%) was purchased from Qingdao Fuslin Chemical Technology Co., Ltd. Expanded graphite (EG, Purity ≥99 wt%) was obtained from Qingdao Xingyuan Colloidal Graphite Co., Ltd. All the chemicals were used without treatment.

Preparation of Rigid Polyurethane Foam Composites

RPUF composites were fabricated by free-rise method; the formulation of the composites was listed in **Table 1**. All the raw materials except PAPI were mixed in a 1,000 ml plastic beaker by high speed mechanical stirrer for 20 s. Then, PAPI was poured into the mixture with vigorous stirring for another 10 s and quickly poured into a mold. The obtained foam was cured at 80°C for 5 h to complete the further polymerization reaction. The samples were cut into suitable size for further characteristics.

TABLE 1 | Formulation of RPUF and FR-RPUF composites.

Sample	LY4110 (php)	PM-200 (php)	LC (php)	AK-8805 (php)	A33 (php)	Water (php)	TEA (php)	ADP (php)	EG (php)
RPUF	100	150	0.5	2	1	2	3	0	0
RPUF/ADP30	100	150	0.5	2	1	2	3	30	0
RPUF/ADP24/EG6	100	150	0.5	2	1	2	3	24	6
RPUF/ADP22.5/EG7.5	100	150	0.5	2	1	2	3	22.5	7.5
RPUF/ADP20/EG10	100	150	0.5	2	1	2	3	20	10
RPUF/ADP18/EG12	100	150	0.5	2	1	2	3	18	12
RPUF/ADP15/EG15	100	150	0.5	2	1	2	3	15	15
RPUF/ADP12/EG18	100	150	0.5	2	1	2	3	12	18
RPUF/ADP10/EG20	100	150	0.5	2	1	2	3	10	20
RPUF/ADP7.5/EG22.5	100	150	0.5	2	1	2	3	7.5	22.5
RPUF/ADP6/EG24	100	150	0.5	2	1	2	3	6	24
RPUF/EG30	100	150	0.5	2	1	2	3	0	30

Measurement and Characterization

Scanning electron microscopy (SEM, JSM-6490LV, JEOL Ltd, Japan) was introduced to observe the cell structure of the specimens with accelerating voltage of 20 kV. Before the observation, the sample surface was coated with a thin conductive layer.

Thermal conductivity was tested according to GB/T 10,297-2015 by thermal conductivity meter (TC3000E, Xiaxi Electronic Technology Co., Ltd, China). The sample size was 30 mm × 30 mm×25 mm. Five parallels for each sample were tested and the average value was obtained.

The apparent density of RPUF composites was measured according to ISO 845-2006. The size of the sample was more than 100 cm^3, and five samples were tested to obtain the average value.

Thermogravimetric analysis (TGA) was conducted by Q5000IR (TA Instruments, United States) thermoanalyzer instrument. 5–10 mg sample was loaded and heated from room temperature to 800°C with heating rate of 20°C/min in N_2 condition. The onset decomposition temperature ($T_{-5\%}$) was defined as the temperature at which 5% of the original weight was lost. The midpoint temperature ($T_{-50\%}$) was defined as the temperature at which 50% of the original weight was lost.

Limiting oxygen index (LOI) test was performed at room temperature by JF-3 oxygen index instrument (Jiangning Analysis Instrument Co., Ltd, China) according to ASTM D2863-97. The sample size was 127 mm × 10 mm × 10 mm.

UL-94 vertical burning test was performed by CZF-3 instrument (Jiangning Analysis Instrument Co., Ltd, China) according to ASTM D3801-96. The specimen dimension was 127 mm × 13 mm × 10 mm.

Combustion properties of the sample were characterized by microscale combustion calorimetry (Govmark, United States) according to ASTM D7309-7. 4–6 mg sample was heated from 100 to 650°C with heating rate of 1°C/s in a stream of N_2 flow of 80 ml/min. The volatile anaerobic thermal degradation products in N_2 gas stream were mixed with 20 ml/min stream of pure O_2 gas prior to entering a 900°C combustion furnace. The MCC data obtained were reproducible to about 3%.

Cone calorimetry test of the samples was performed by cone calorimeter (Fire Testing Technology, United Kingdom) according to ISO 5660. The sample with dimension of 100 mm × 100 mm × 4 mm was wrapped with aluminum foil and exposed horizontally to 35 kW/m^2 external heat flux.

Thermogravimetric analysis-Fourier Transform Infrared Spectrometer (TG-FTIR) was conducted by using Q5000IR (TA Instruments, United States) thermoanalyzer instrument which was connected with Nicolet 6700 FTIR spectrophotometer (Thermo Scientific Nicolet, United States). About 5–10 mg of the sample was put in an alumina crucible and heated from 30 to 700°C. The heating rate was 20°C/min in nitrogen atmosphere with flow rate of 70 ml/min.

Char residues of the sample were obtained by calcining the composites in 600 C for 10 min. The morphology of the char residue was investigated by scanning electron microscopy (JSM-6490LV, JEOL Ltd, Japan) with accelerating voltage of 20 kV. The specimens were sputter-coated with a conductive layer.

X-ray photoelectron spectroscopy (XPS) with a VG Escalab Mark II spectrometer (Thermo-VG Scientific Ltd. United States) using Al Ka excitation radiation (hν = 1,253.6 eV) was introduced to investigate the char residues.

Structural Characterization

The RPUF and FR-RPUF composites exhibit different morphologies with various formulations (**Table 1**). The surface microstructure of polyurethane foams can be observed by scanning electron microscope (SEM). As shown in **Figure 1A**, the pure RPUF sample shows the honeycomb obturator bubble structures with relatively smooth surface, and the diameters range from 500 to 800 μm. After the addition of EG, the bubbles RPUF/EG30 are relatively complete, and the bubble size is obviously reduced compared with pure sample (**Figure 1B**). Meanwhile, RPUF/EG30 presents better pore size distribution, which may be due to the nucleation effect of EG. In addition, some open pore structures can be observed in a few bubbles, because of local internal stress and unbalanced foam growth (He et al., 2020). For RPUF/ADP30, the regularity and integrity of bubbles are

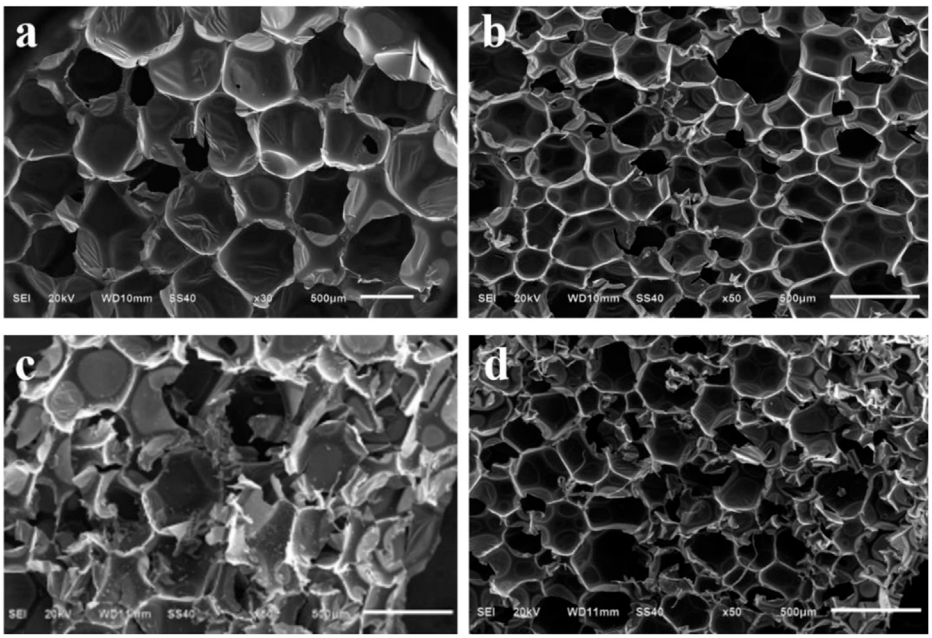

FIGURE 1 | SEM images of RPUF and FR-RPUF composite: **(A)** RPUF; **(B)** RPUF/EG30; **(C)** RPUF/ADP30; **(D)** RPUF/ADP15/EG15.

TABLE 2 | Apparent density and thermal conductivity of RPUF and FR-RPUF composites.

Sample	ρ (kg/m^3)	λ (W/m·k)
RPUF	58.8	0.0392
RPUF/ADP30	58.0	0.0468
RPUF/ADP24/EG6	63.7	0.0419
RPUF/ADP22.5/EG7.5	64.0	0.0438
RPUF/ADP20/EG10	60.2	0.0439
RPUF/ADP18/EG12	58.8	0.0443
RPUF/ADP15/EG15	57.3	0.0446
RPUF/ADP12/EG18	57.1	0.0450
RPUF/ADP10/EG20	57.3	0.0452
RPUF/ADP7.5/EG22.5	52.7	0.0466
RPUF/ADP6/EG24	51.2	0.0474
RPUF/EG30	69.3	0.0467

significantly reduced, and the unevenly dispersed ADP particles are clearly observed on the surface of the bubbles (**Figure 1C**). This result indicates the poor compatibility between ADP and RPUF, and it is not beneficial to the improvement of flame retardant efficiency and mechanical properties of RPUF. When combining ADP and EG together in RPUF, the bubble pore size is further reduced with lower morphology regularity compared with RPUF/EG30. Meanwhile, there appears obvious pore collapse and surface curling phenomenon, due to the joint action of ADP and EG. However, compared to the sample with ADP alone, no obvious exposed ADP particles are observed (**Figure 1D**). The density of RPUF usually has an important influence on the performance of the material. The densities of rigid foam with different components were summarized in **Table 2**. The density of neat RRUF was 58.8 kg/m^3, and the addition of ADP and EG changed the density of foams. When ADP and EG were combined together in RPUF, the density of foam decreases with the increase of EG content. However, when 30 php EG was added, the foam density increased significantly to 69.3 kg/m^3.

Thermal Conductivity

For RPUF, thermal insulation is an important performance index. Thermal insulation performance will be affected by many factors, such as the type of foaming agent, cell size, ratio of open and closed cells, and foam density (Debski et al., 2001). The influence of ADP and EG on thermal conductivity was also listed in **Table 2**. It can be seen that the thermal conductivity of pure RPUF was as low as 0.0392 W/m·K. With the addition of different proportions of ADP and EG in RPUF, the thermal conductivity of all FR-PURF composites increased. It was worth noting that the thermal conductivity increased, as the content of EG in RPUF increased. When the addition of ADP and EG were 6 and 24 php, respectively, the thermal conductivity of RPUF/ADP6/EG24 increased to the maximum 0.0474 W/mk. The increase may result from the shrinkage of the cells caused by EG.

Thermal Stability

RPUF usually exhibits an anaerobic thermal decomposition process during combustion; thus the thermal stability of RPUF was investigated by TGA in nitrogen atmosphere (**Figure 2**). And some important parameters such as the temperatures at a specific weight loss ($T_{-5\%}$ and $T_{-50\%}$), the temperature at maximum mass loss rate (T_{max}), and the residues at 800°C are listed in **Table 3**. As shown in **Figure 2**, the pure RPUF presents the two-stage thermal degradation process. The first stage occurred at around 180–325°C with 34.3% weight loss, caused by the decomposition of hard segments in polyurethane molecular chains, producing polyols,

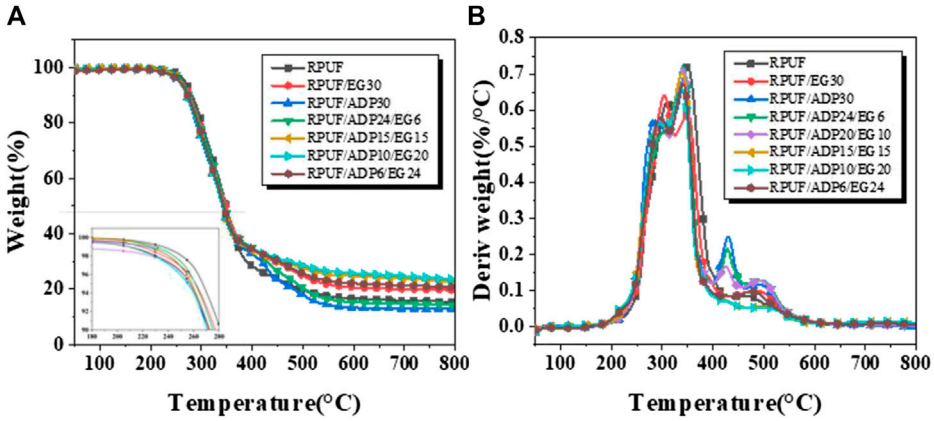

FIGURE 2 | (A) TGA and **(B)** DTG curves of RPUF and FR-RPUF composites under N_2.

TABLE 3 | TGA results of RPUF and FR-RPUF composites under N_2. Flame retardant performance.

Samples	$T_{-5\%}$ (°C)	$T_{-50\%}$ (°C)	T_{max} (°C)	Residue (wt%)
RPUF	267.3	348.4	350.6	15.54
RPUF/EG30	261.7	348.1	304.0	19.72
RPUF/ADP24/EG6	261.2	345.4	340.9	14.44
RPUF/ADP20/EG10	257.4	341.7	340.9	14.27
RPUF/ADP15/EG15	258.6	341.3	338.9	22.71
RPUF/ADP10/EG20	255.4	341.2	338.3	23.58
RPUF/ADP6/EG24	257.0	343.1	340.2	20.78
RPUF/ADP30	258.8	341.0	342.8	12.97

isocyanates carbon dioxide, amines, and so on. Corresponding to a weight loss of 49%, the second stage occurred at temperature between 325 and 590°C and was attributed to the decomposition of soft polyol segments. For FR-RPUF, the $T_{-5\%}$ of all samples were decreased to a certain extent, due to breaking of weak bonds and the earlier degradation of polyurethane molecular, which resulted from acid substance released from the EG and ADP. In particular, the $T_{-5\%}$ decreased with the increasing ADP contents. However, the earlier degradation of flame retardant was beneficial to the improvement of flame retardant performance for FR-RPUF composites. It is worth noting that ADP and EG had different effects on the thermal degradation process of RPUF. With the increase of ADP content, a new peak at 400–550°C gradually appeared on the DTG curve of the RPUF/ADP30, resulting in 20% weight loss approximately, due to the formation of volatile phosphinate compounds (Zhan et al., 2015). Also, the $T_{-50\%}$ for samples containing ADP were slightly decreased. Though EG component exhibits no obvious influence on $T_{-50\%}$, it causes the significant reduction on T_{max}. Additionally, it is notable that the T_{max} of RPUF/EG30 was lower than $T_{-50\%}$ at a great extent, indicating more foam matrix can be retained during combustion. In fact, the char residues of RPUF/EG30 are 19.72%, which is much higher than 15.54% of RPUF and 12.97% of RPUF/ADP30. It has been reported that a low-density worm-like insulation layer would be produced steadily on the surface of matrix, when EG is activated during heating process, which effectively inhibits the transfer of heat

TABLE 4 | LOI and UL-94 test results of RPUF and FR-RPUF composites.

Sample	LOI	UL-94. 10.0 mm bar		
	vol%	t_1/t_2[a](s)	Dripping	Rating
RPUF	18.8	28.2/0	N	NR[b]
RPUF/ADP30	23.0	16.4/0	N	V-1
RPUF/ADP24/EG6	23.2	19.9/0	N	V-1
RPUF/ADP22.5/EG7.5	23.9	18.2/0	N	V-1
RPUF/ADP20/EG10	24.5	17.9/0	N	V-1
RPUF/ADP18/EG12	24.3	18.3/0	N	V-1
RPUF/ADP15/EG15	24.5	18.2/0	N	V-1
RPUF/ADP12/EG18	25.3	16.8/0	N	V-1
RPUF/ADP10/EG20	25.9	14.2/0	N	V-1
RPUF/ADP7.5/EG22.5	25.3	12.2/0	N	V-1
RPUF/ADP6/EG24	25.7	12.1/0	N	V-1
RPUF/EG30	25.2	12.3/0	N	V-1

[a]*t_1 and t_2, average combustion times after the first and the second applications of the flame.*
[b]*NR, no rating.*

and substances (Acuña et al., 2020). Taking all parameters into considerations, RPUF/ADP10/EG20 shows the best thermal stability with the highest residues and the lowest onset decomposition temperature, which would promote the formation of protective layer in a fire.

The flame retardant properties of pure RPUF and FR-RPUF were firstly evaluated by limiting oxygen index (LOI) test, as shown in **Table 4**. The LOI value of pure RPUF is 18.8 vol%. With the addition of 30 php of ADP, the LOI value of RPUF/ADP30 increased to 23.0 vol%. After adding 30 php of EG, the LOI value of RPUF/EG30 can reach 25.2 vol%, higher than the composites modified by ADP alone. When EG and ADP are added at the same time, the LOI values of RPUF are obviously higher than that of RPUF/ADP30. However, the samples show different LOI values with different EG and ADP additions. Among them, the LOI value of RPUF/ADP10/EG20 can reach the maximum 25.9 vol%. It is worth noting that RPUF/ADP12/EG (Akdogan et al., 2020), RPUF/ADP10/EG20, RPUF/ADP7.5/EG22.5, and RPUF/ADP6/EG24 composites have greater LOI values

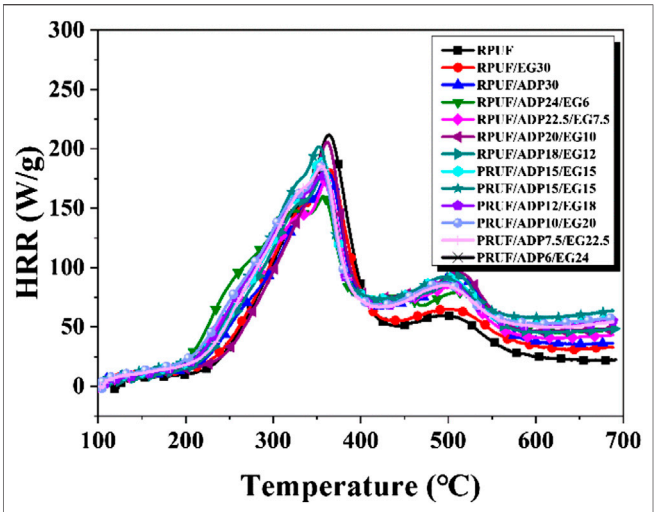

FIGURE 3 | MCC results of RPUF and FR-RPUF composites.

compared with RPUF/ADP30 and RPUF/EG30. These results indicate that there exists a good synergistic flame retardant effect between ADP and EG. Vertical burning test (UL 94) is used to evaluate the flame retardant performance of RPUF and FR-RPUF composites. As shown in **Table 4**, compared with no rating of the pure RPUF, all FR-RPUF exhibited V-1 rating, indicating the improved flame retardancy of the composites.

As a simple screening method, MCC analysis was performed, where only a small amount of samples was needed to investigate the combustion of the RPFU and FR-RPUF composite (Chu et al., 2018). Heat release rate (HRR) curves can be obtained from MCC and were depicted in **Figure 3**. Meanwhile, as an important parameter to evaluate the flame retardancy of materials, peak heat release rate (PHRR) was summarized in **Table 5**. Compared with pure RPUF, all modified FR-RPUF exhibits lower PHRR values. In comparison with the 211.86 W/g of pure RPUF, the PHRR values of RPUF/EG30 and RPUF/ADP30 were reduced to 180.15 and 179.61 W/g, respectively, with the addition of 30 php of EG and ADP. When EG and ADP were combined together in RPUF, the PHRR values of the samples presented a certain difference under different component contents. Among them, RPUF/ADP24/EG6 had the lowest PHRR value of 159.85 W/g, which was 52.01 W/g lower than that of pure RPUF.

The combustion properties of pure RPUF and FR-RPUF were tested through cone calorimeter. HRR and total heat release (THR) curves were depicted in **Figure 4**, and the data were listed in **Table 5**. As shown in **Figure 4A**, pure RPUF reached the peak of maximum heat release rate soon after ignition (298.28 kW/m^2). All FR-RPUF exhibited a different heat release behavior from pure RPUF. Compared with pure RPUF, the PHRR of RPUF/EG30 was reduced to 161.27 kW/m^2, experiencing 45.93% of decrement. The reason why RPUF with addition of EG had such a low PHRR was as follows: When heated, EG expanded and a large amount of worm-like carbon layer was formed, which served as a physical barrier in the condensed phase and gas phase of the combustion zone. Moreover, the large amount of incombustible gas formed by the expansion would dilute the concentration of the fuel. However, RPUF modified with EG had longer flaming combustion time, due to the delayed release of combustible gases in the presence of EG. The THR of RPUF/EG30 was 23.08 MJ/m^2, decreased by 18.65% compared with the pure RPUF. The reduction in THR was not as great as that in PHRR. That was because EG modified RPUF possessed a higher density than pure RPUF; thus more fuel would be contained in the combustion process. Two peaks can be seen in the HRR curves of some samples. This may be ascribed to the expansion of the sample during the combustion process, which shortened the distance between the sample surface and the heating coil. Thus, higher thermal radiation can be received by samples, and the combustion will release more heat.

Gaseous Phase Analysis

The volatile products of RPUF and FR-RPUF composites during the pyrolysis process were investigated by TG-IR. The Gram-Schmidt (GS) curves and the absorbance intensity of the typical gas products were shown in **Figure 5A**. The absorbance intensity of RPUF composites was significantly reduced compared with pure RPUF, with the addition of EG and ADP. Moreover, RPUF/ADP15/EG15 showed lower absorbance intensity than RPUF/EG and RPUF/ADP, indicating the synergistic smoke suppression effect between the EG and ADP. The absorption intensities of released CO_2 compounds and hydrocarbons were presented in **Figure 5E**, and the intensity of RPUF was lower than that of RPUF/EG30. This may be due to the structural characteristics of expandable graphite itself, which made it easy to release volatile hydrocarbons during combustion. However, due to the expandability of expanded graphite and its high temperature resistance, expandable graphite expanded rapidly at high temperatures. At the same time, the produced expanded graphite materials covered the surface of the substrate, isolating heat radiation and oxygen. The acid radicals inside the interlayer can be released during expansion, which also promoted the carbonization of the substrate. When combined with ADP in RPUF, the thermal decomposition products of ADP had a strong dehydration effect, and the covered polymer surface was carbonized to form a carbon film. Thus, a good flame

TABLE 5 | PHRR and THR from MCC and cone.

Sample	PHRR (W/g, MCC)	PHRR (kW/m^2, cone)	THR (MJ/m^2)
RPUF	211.86	298.28	28.37
RPUF/ADP30	179.61	322.48	21.31
RPUF/ADP24/EG6	159.85	296.06	34.30
RPUF/ADP22.5/EG7.5	172.80	—	—
RPUF/ADP20/EG10	205.50	372.50	33.64
RPUF/ADP18/EG12	180.16	—	—
RPUF/ADP15/EG15	191.88	323.57	32.55
RPUF/ADP12/EG18	201.71	—	—
RPUF/ADP10/EG20	177.87	286.30	35.10
RPUF/ADP7.5/EG22.5	185.35	—	—
RPUF/ADP6/EG24	185.41	310.79	37.84
RPUF/EG30	180.15	161.27	23.08

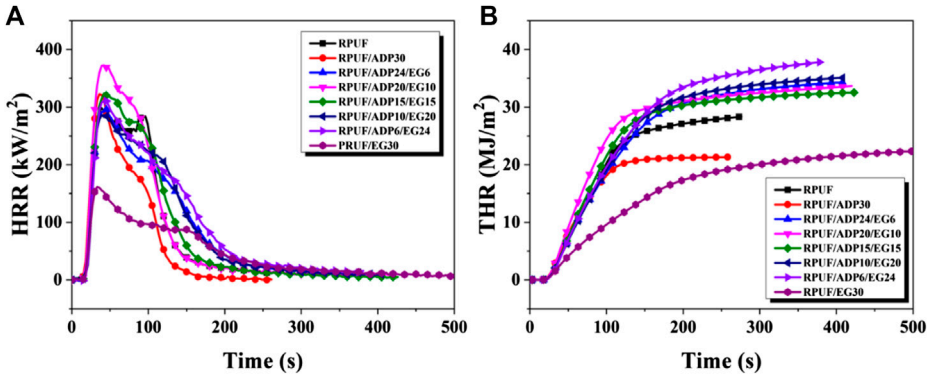

FIGURE 4 | HRR **(A)** and THR **(B)** curves vs time of RPUF and FR-RPUF composites.

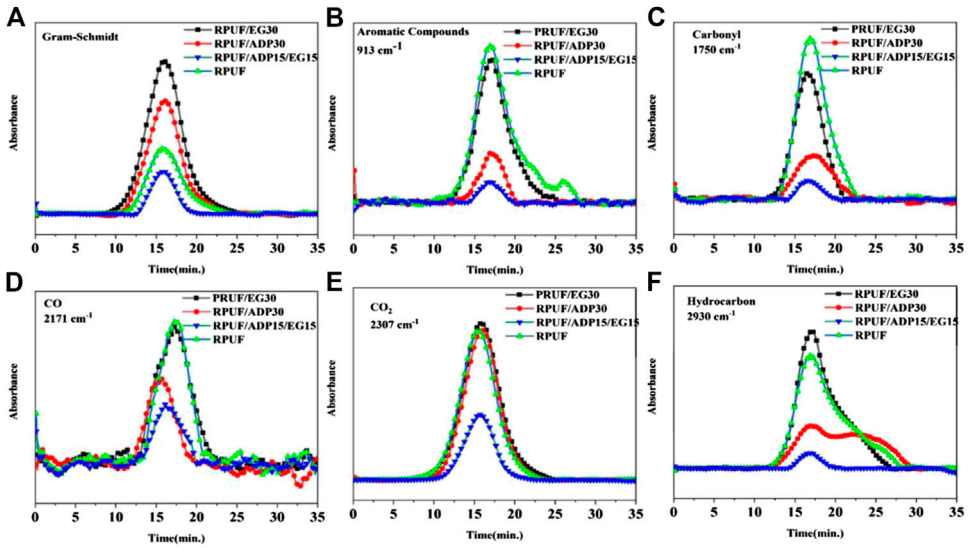

FIGURE 5 | Absorbance of gaseous products of RPUF and FR-RUUF composites versus time: **(A)** Gram-schmidt; **(B)** aromatic compounds; **(C)** carbonyl; **(D)** CO; **(E)** CO_2; **(F)** hydrocarbon.

retardant effect can be achieved through this synergistic flame retardant method. Furthermore, the decrease in the strength of the aromatic compound may imply a reduction in the yield of aromatic volatiles, which lead to suppression of smoke particles that were formed by these condensed aromatic fragments. Moreover, poisonous gas products such as CO and carbonyl can threaten the safety of human life seriously (Chu et al., 2018; Shi et al., 2019; Liu et al., 2020; Shi et al., 2020; Chu et al., 2021). Therefore, it is important to reduce the release of these toxic substances. The corresponding absorption intensities of CO and carbonyl were given in **Figures 5C,D**, respectively. With the addition of EG and ADP, a significant decrease in absorbance can be achieved and RPU/ADP15/EG15 had the lowest intensity. This indicates that the combination of EG and ADP can effectively inhibit the burning toxicity of the polymer. In addition, the polymer added with ADP would also produce an expanded carbon layer during the combustion process to achieve the effects of heat and oxygen insulation and further prevented the spread of surface flames, playing a key role in flame retardancy (Qiu et al., 2019).

Condensed Phase Analysis

SEM was used to further characterize the external and internal char residues of four different polyurethane foams, which can further explain their different performance in flame retardancy (Xu et al., 2020). As shown in **Figure 6**, there were many carbon micron spheres on the surface of residues of pure RPUF, without a continuous and dense char layer. The internal carbon layer had obvious rupture, which had a weak inhibition effect on the release of fuel from the matrix and the transfer of heat to the matrix. Finally, the pure RPUF showed poor fire safety performance. In contrast, RPUF/ADP30 presented a much smaller number of carbon micron spheres on the surface of residual. A relatively continuous char layer can be formed on the surface, and the char layer inside was also more compact. Compared with the pure

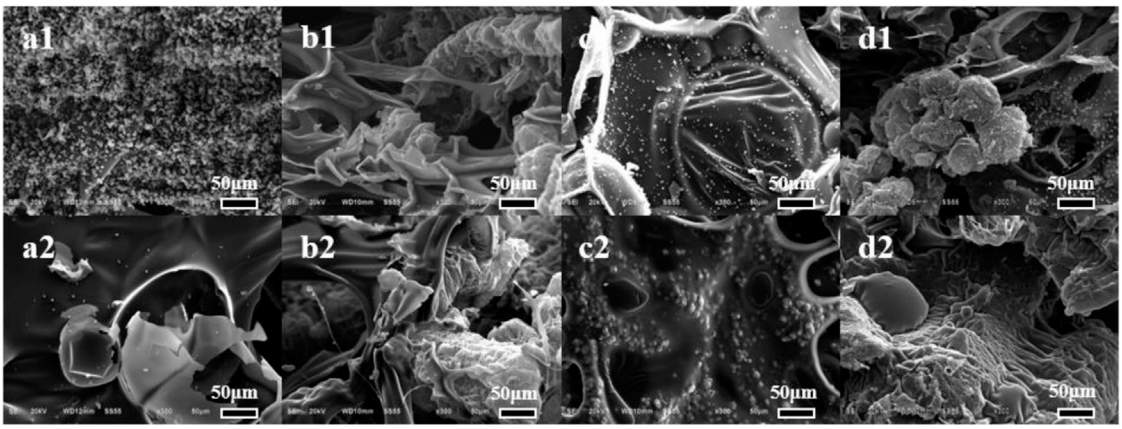

FIGURE 6 | SEM images of the external and internal char residues of RPUF and FR-RPUF composites: **(A)** RPUF; **(B)** RPUF/EG30; **(C)** RPUF/ADP30; **(D)** RPUF/ADP15/EG15.

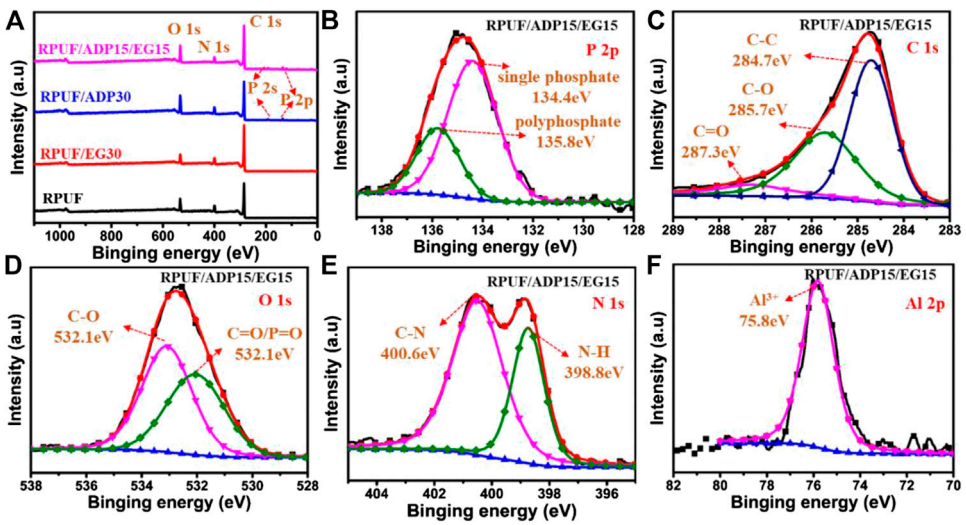

FIGURE 7 | (A) XPS survey spectrum of the residual char for RPUF and its nanocomposites after cone tests; high-resolution, **(B)** P 2p, **(C)** C 1s, **(D)** O 1s, **(E)** N 1s, and **(F)** Al 2p XPS spectra of RPUF/ADP15/EG15.

RPUF, the flame retardant performance of RPUF/ADP30 was significantly improved. However, some obvious holes were observed on the surface of char layers, which limited the suppression effect of mass and heat transfer. In the case of ADP and EG combined, there were also carbon micron spheres on the surface of the external char layer. The specific worm-like char layer formed by expandable graphite had obvious rupture, which was not conducive to the improvement of flame retardant performance, while the internal char layer presented dense and continuous morphology.

For the RPUF with only EG added, the internal and external morphology were similar. On outside, there appeared continuous and relatively loose worm-like carbon layer, and the formed char framework was continuously dense, without any carbon micron ball. Meanwhile, the worm-like char layer and char layer framework inside were more dense, which had an advantage in improving the flame retardant performance.

The more diversified information about the surface composition and chemical state of the residual chars can be offered by the XPS analysis. As shown in **Figure 7A**, the XPS survey spectra of RPUF and RPUF/EG30 were composed of C, N, and O elements, but there were additional P elements in the residual char of RPUF/ADP30 and RPUF/ADP15/EG15 nanocomposites. Moreover, the O content in the surface char layer of RPUF/ADP30 and RPUF/ADP15/EG15 was 15.9 and 13.1%, respectively, higher than that of RPUF and RPUF/EG30 (12.1 and 8.4%), respectively. This result is due to the decomposition of ADP to produce POx during combustion process, which can promote carbon formation (Zhou et al., 2020). **Figures 7B–F** showed the P 2p, C 1s, O 1s, N 1s, and Al 2p spectra of the external char of RPUF/ADP15/EG15. As shown in the P 2p

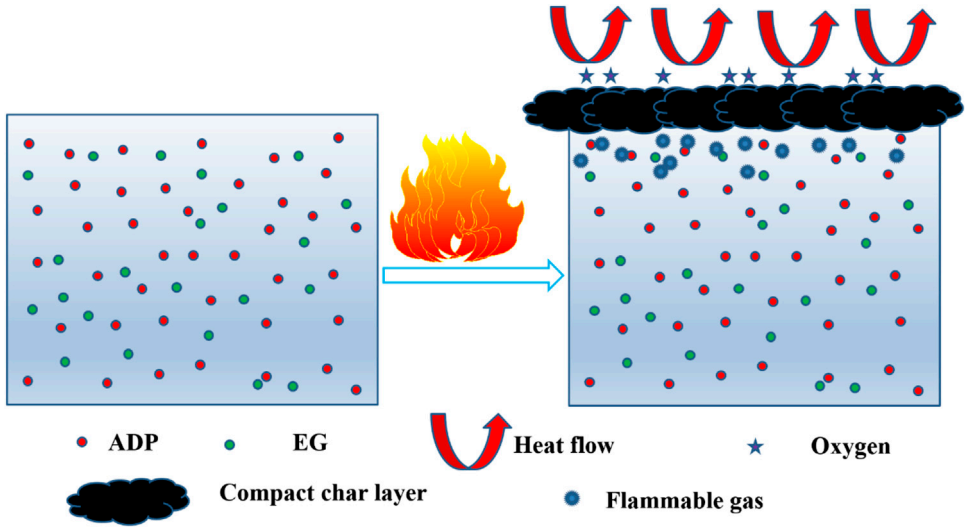

FIGURE 8 | Schematical illustration of flame retardant mechanism for RPUF/ADP/EG composites.

spectrum, two peaks appear in the 134.4 and 135.8 eV, which was attributed to single phosphate and pyrophosphate, respectively, revealing the formation of cross-linked phosphorus oxide compounds (Zhou et al., 2020). As shown in C 1s spectrum, the C 1s peaks can be deconvoluted into three peaks at 284.7, 285.7, and 287.3 eV corresponding to C-C, C-O, and C=O bonds, respectively. Correspondingly, C-O and C=O can also be found in O 1s spectrum, and the peak corresponding to C=O also corresponds to P=O in phosphate groups (Qiu et al., 2020). Two peaks at 398.8 and 400.6 eV assigned to N-H and C-N bondings were found in the N 1s spectrum (Qiu et al., 2019), owing to the carbonitride after the decomposition of RPUF. A peak at 75.8 eV is found in the Al 2p spectrum, representing phosphate and/or aluminum pyrophosphate (Tang et al., 2013).

Mechanism Consideration

Based on the above investigation, possible fire retarded mechanism of RPUF/ADP/EG composites was proposed and the corresponded schematical illustration was presented in **Figure 8**. As being ignited, the fire usually started on the surface of the composites. EG particles could expand and form worm-like structure with some holes by the released SO_2 or NO_2 (Wang et al., 2011). ADP particles decomposed into oligomers of phosphinates, diethylphosphinic acid, and aluminum phosphate (Orhan et al., 2012; Kaya and Hacaloglu, 2014). Oligomers of phosphinates further decomposed into P and PO, which could quench H· and HO· in gas phase. Diethylphosphinic acid could further promote polyurethane chain into char and reduce the production of combustible gas. The char combined with aluminum phosphate to form carbon film and cover on the surface of worm-like structure, significantly enhancing compactness of the char residue. The compact char residue could significantly inhibit heat and substance transfer and thus effectively suppress burning of underlying materials and obviously enhance fire retarding of RPUF/ADP/EG composites. Thus, ADP/EG systems mostly play their role by gas-solid flame retardant mechanism.

CONCLUSION

This work investigated the effect of EG and ADP on the structure, thermal conductivity, thermal stability, and flame retardant performance of RPUF and FR-RPUF. When the addition of ADP and EG was 6 and 24 php, respectively, the thermal conductivity of RPUF/ADP6/EG24 increased to the maximum 0.0474 W/m·k. The increase may be caused by the shrinkage of the cells caused by EG. For FR-RPUF, the thermal stability decreased with the increasing ADP contents, and the char residues increased as EG contents increased. Meanwhile, the results in flame retardant performance indicated the addition of ADP and EG can improve the flame retardancy of RPUF, and there existed a good synergistic flame retardant effect between ADP and EG. The flame retardant mechanism was investigated from gaseous and condensed phase, respectively.

DATA AVAILABILITY STATEMENT

The original contributions presented in the study are included in the article/Supplementary Material; further inquiries can be directed to the corresponding author.

AUTHOR CONTRIBUTIONS

YH: Formal analysis, Investigation, Visualization, Writing-original draft. ZZ: Formal analysis, Investigation, Writing & reviewing. SL: Conceptualization, Resources, Supervision. DY: Methodology, Project administration, Writing-reviewing & editing. SZ: Investigation, Writing-original draft. YH: Investigation, Writing-original draft.

REFERENCES

Acuña, P., Lin, X., Calvo, M. S., Shao, Z., Pérez, N., Villafañe, F., et al. (2020). Synergistic effect of expandable graphite and phenylphosphonic-aniline salt on flame retardancy of rigid polyurethane foam. *Polym. Degrad. Stabil.*, 179, 109274. doi:10.1016/j.polymdegradstab.2020.109274

Akdogan, E., Erdem, M., Ureyen, M. E., and Kaya, M. (2020). Synergistic effects of expandable graphite and ammonium pentaborate octahydrate on the flame-retardant, thermal insulation, and mechanical properties of rigid polyurethane foam. *Polym. Compos.*, 41 (5), 1749–1762. doi:10.1002/pc.25494

Barkoula, N. M., Alcock, B., Cabrera, N. O., and Peijs, T. (2008). Flame-retardancy properties of intumescent ammonium poly(phosphate) and mineral filler magnesium hydroxide in combination with graphene. *Polym. Polym. Compos.* 16 (2), 101–113. doi:10.1002/pc

Bhoyate, S., Ionescu, M., Kahol, P. K., and Gupta, R. K. (2019). Castor-oil derived nonhalogenated reactive flame-retardant-based polyurethane foams with significant reduced heat release rate. *J. Appl. Polym. Sci.* 136 (13), 1–7. doi:10.1002/app.47276

Chen, Y., Luo, Y., Guo, X., Chen, L., and Jia, D. (2020). The synergistic effect of ionic liquid-modified expandable graphite and intumescent flame-retardant on flame-retardant rigid polyurethane foams. *Materials* 13 (14), 3095. doi:10.3390/ma13143095

Chen, Y., Luo, Y., Guo, X., Chen, L., Xu, T., and Jia, D. (2019). Structure and flame-retardant actions of rigid polyurethane foams with expandable graphite. *Polymers* 11 (4), 686. doi:10.3390/polym11040686

Cheng, J., Niu, S., Ma, D., Zhou, Y., Zhang, F., Qu, W., et al. (2020). Effects of ammonium polyphosphate microencapsulated on flame retardant and mechanical properties of the rigid polyurethane foam. *J. Appl. Polym. Sci.* 137 (48), 2–9. doi:10.1002/app.49591

Chu, F., Xu, Z., Zhou, Y., Zhang, S., Mu, X., Wang, J., et al. (2021). Hierarchical core–shell TiO2@LDH@Ni(OH)2 architecture with regularly-oriented nanocatalyst shells: towards improving the mechanical performance, flame retardancy and toxic smoke suppression of unsaturated polyester resin. *Chem. Eng. J.* 405, 126650. doi:10.1016/j.cej.2020.126650

Chu, F., Yu, X., Hou, Y., Mu, X., Song, L., and Hu, W. (2018). A facile strategy to simultaneously improve the mechanical and fire safety properties of ramie fabric-reinforced unsaturated polyester resin composites. *Compos. Appl. Sci. Manuf.* 115, 264–273. doi:10.1016/j.compositesa.2018.10.006

Chu, F., Zhang, D., Hou, Y., Qiu, S., Wang, J., Hu, W., et al. (2018). Construction of hierarchical natural fabric surface structure based on two-dimensional boron nitride nanosheets and its application for preparing biobased toughened unsaturated polyester resin composites. *ACS Appl. Mater. Interfaces* 10 (Issue 46), 40168–40179. doi:10.1021/acsami.8b15355

Debski, K., Magiera, J., and Pielichowski, J. (2001). The effect of the structure of rigid polyurethane foams blown with a hydrocarbon blowing agent on foam's apparent thermal conductivity. *Polimery/Polymers* 46 (9), 631–637. doi:10.14314/polimery.2001.631

Han, S., Zhu, X., Chen, F., Chen, S., and Liu, H. (2020). Flame-retardant system for rigid polyurethane foams based on diethyl bis(2-hydroxyethyl) aminomethylphosphonate and *in-situ* exfoliated clay. *Polym. Degrad. Stabil.* 177, 109178. doi:10.1016/j.polymdegradstab.2020.109178

He, W., Kang, P., Fang, Z., Hao, J., Wu, H., Zhu, Y., et al. (2020). Flow reactor synthesis of bio-based polyol from soybean oil for the production of rigid polyurethane foam. *Ind. Eng. Chem. Res.* 59 (39), 17513–17519. doi:10.1021/acs.iecr.0c01175

Hejna, A., Kosmela, P., Kirpluks, M., Cabulis, U., Klein, M., Haponiuk, J., et al. (2018). Structure, mechanical, thermal and fire behavior assessments of environmentally friendly crude glycerol-based rigid polyisocyanurate foams. *J. Polym. Environ.* 26 (5), 1854–1868. doi:10.1007/s10924-017-1086-2

Kaya, H., and Hacaloglu, J. (2014). Thermal degradation of polylactide/aluminium diethylphosphinate. *J. Anal. Appl. Pyrol.* 110 (1), 155–162. doi:10.1016/j.jaap.2014.08.015

Li, P., Xiao, Z., Chang, C., Zhao, S., and Xu, G. (2020). Efficient synthesis of biobased glycerol levulinate ketal and its application for rigid polyurethane foam production. *Ind. Eng. Chem. Res.* 59 (39), 17520–17528. doi:10.1021/acs.iecr.9b06038

Liu, C., Wu, W., Shi, Y., Yang, F., Liu, M., Chen, Z., et al. (2020). Creating MXene/reduced graphene oxide hybrid towards highly fire safe thermoplastic polyurethane nanocomposites. *Compos. B Eng.*, 203 (October), 108486. doi:10.1016/j.compositesb.2020.108486

Liu, L., and Wang, Z. (2018). High performance nano-zinc amino-tris-(methylenephosphonate) in rigid polyurethane foam with improved mechanical strength, thermal stability and flame retardancy. *Polym. Degrad. Stabil.* 154, 62–72. doi:10.1016/j.polymdegradstab.2018.05.023

Orhan, T., Isitman, N. A., Hacaloglu, J., and Kaynak, C. (2012). Thermal degradation of organophosphorus flame-retardant poly(methyl methacrylate) nanocomposites containing nanoclay and carbon nanotubes. *Polym. Degrad. Stabil.* 97 (3), 273–280. doi:10.1016/j.polymdegradstab.2011.12.020

Pan, Y., Song, L., Wang, W., and Zhao, H. (2020). Polydimethylsiloxane wrapped aluminum diethylphosphinate for enhancing the flame retardancy of polyamide 6. *J. Appl. Polym. Sci.*, 137 (35), 1–8. doi:10.1002/app.49027

Qiu, S., Zhou, Y., Ren, X., Zou, B., Guo, W., Song, L., et al. (2020). Construction of hierarchical functionalized black phosphorus with polydopamine: a novel strategy for enhancing flame retardancy and mechanical properties of polyvinyl alcohol. *Chem. Eng. J.*, 402, 126212. doi:10.1016/j.cej.2020.126212

Qiu, S., Zhou, Y., Zhou, X., Zhang, T., Wang, C., Yuen, R. K. K., et al. (2019). Air-Stable polyphosphazene-functionalized few-layer black phosphorene for flame retardancy of epoxy resins. *Small*, 15 (10), e1805175. doi:10.1002/smll.201805175

Shi, Y., Liu, C., Duan, Z., Yu, B., Liu, M., and Song, P. (2020). Interface engineering of MXene towards super-tough and strong polymer nanocomposites with high ductility and excellent fire safety. *Chem. Eng. J.* 399 (June), 125829. doi:10.1016/j.cej.2020.125829

Shi, Y., Liu, C., Liu, L., Fu, L., Yu, B., Lv, Y., et al. (2019). Strengthening, toughing and thermally stable ultra-thin MXene nanosheets/polypropylene nanocomposites via nanoconfinement. *Chem. Eng. J.* 378, 122267. doi:10.1016/j.cej.2019.122267

Tang, G., Liu, X., Zhou, L., Zhang, P., Deng, D., and Jiang, H. (2020). Steel slag waste combined with melamine pyrophosphate as a flame retardant for rigid polyurethane foams. *Adv. Powder Technol.* 31 (1), 279–286. doi:10.1016/j.apt.2019.10.020

Tang, G., Wang, X., Xing, W., Zhang, P., Wang, B., Hong, N., et al. (2012). Thermal degradation and flame retardance of biobased polylactide composites based on aluminum hypophosphite. *Ind. Eng. Chem. Res.* 51 (37), 12009–12016. doi:10.1021/ie3008133

Tang, G., Zhang, R., Wang, X., Wang, B., Song, L., Hu, Y., et al. (2013). Enhancement of flame retardant performance of bio-based polylactic acid composites with the incorporation of aluminum hypophosphite and expanded graphite. *J. Macromol. Sci., Pure Appl. Chem.* 50 (2), 255–269. doi:10.1080/10601325.2013.742835

Tang, G., Zhou, L., Zhang, P., Han, Z., Chen, D., Liu, X., et al. (2020). Effect of aluminum diethylphosphinate on flame retardant and thermal properties of rigid polyurethane foam composites. *J. Therm. Anal. Calorim.*, 140 (2), 625–636. doi:10.1007/s10973-019-08897-z

Wang, B., Hu, S., Zhao, K., Lu, H., Song, L., and Hu, Y. (2011). Preparation of polyurethane microencapsulated expandable graphite, and its application in ethylene vinyl acetate copolymer containing silica-gel microencapsulated ammonium polyphosphate. *Ind. Eng. Chem. Res.*, 50 (20), 11476–11484. doi:10.1021/ie200886e

Wang, C., Wu, Y., Li, Y., Shao, Q., Yan, X., Han, C., et al. (2018). Flame-retardant rigid polyurethane foam with a phosphorus-nitrogen single intumescent flame retardant. *Polym. Adv. Technol.* 29 (1), 668–676. doi:10.1002/pat.4105

Wang, S. X., Zhao, H. B., Rao, W. H., Huang, S. C., Wang, T., Liao, W., et al. (2018). Inherently flame-retardant rigid polyurethane foams with excellent thermal insulation and mechanical properties. *Polymer*, 153, 616–625. doi:10.1016/j.polymer.2018.08.068

Wang, S., Yang, X., Li, Z., Xu, X., Liu, H., Wang, D., et al. (2020). Novel eco-friendly maleopimaric acid based polysiloxane flame retardant and application in rigid polyurethane foam. *Compos. Sci. Technol.* 198, 108272. doi:10.1016/j.compscitech.2020.108272

Xu, Z., Duan, L., Hou, Y., Chu, F., Jiang, S., Hu, W., et al. (2020). The influence of carbon-encapsulated transition metal oxide microparticles on reducing toxic gases release and smoke suppression of rigid polyurethane foam composites. *Composites Part A: applied science and manufacturing* 131, 105815. doi:10.1016/j.compositesa.2020.105815

Zhan, Z., Xu, M., and Li, B. (2015). Synergistic effects of sepiolite on the flame retardant properties and thermal degradation behaviors of polyamide 66/aluminum diethylphosphinate composites. *Polym. Degrad. Stabil.* 117, 66–74. doi:10.1016/j.polymdegradstab.2015.03.018

Zhou, Q., Gong, K., Zhou, K., Zhao, S., and Shi, C. (2019). Synergistic effect between phosphorus tailings and aluminum hypophosphite in flame-retardant thermoplastic polyurethane composites. *Polym. Adv. Technol.*, 30 (9), 2480–2487. doi:10.1002/pat.4695

Zhou, Y., Chu, F., Qiu, S., Guo, W., Zhang, S., Xu, Z., et al. (2020). Construction of graphite oxide modified black phosphorus through covalent linkage: an efficient strategy for smoke toxicity and fire hazard suppression of epoxy resin. *J. Hazard Mater.* 399 (May), 123015. doi:10.1016/j.jhazmat.2020.123015

Conflict of Interest: YH, SL, DY, SZ, and YH were employed by company China Construction Fifth Engineering Division Co., Ltd.

The remaining authors declare that the research was conducted in the absence of any commercial or financial relationships that could be construed as a potential conflict of interest.